Journal of South American Earth Sciences 109 (2021) 103254

Contents lists available at ScienceDirect

Journal of South American Earth Sciences

journal homepage: www.elsevier.com/locate/jsames

Glacier retreat and associated processes since the Last Glacial Maximum in the Lejiamayu valley, Peruvian Andes

Adam Emmer[a,*], Melaine Le Roy[b,c], Ashim Sattar[d,j], Bijeesh K. Veettil[e,k], Jesús Alcalá-Reygosa[f], Néstor Campos[g], Jakub Malecki[h], Alejo Cochachin[i]

[a] *University of Graz, Institute of Geography and Regional Science, 8010, Graz, Austria*
[b] *University of Geneva, Institute for Environmental Sciences, Climate Change Impacts and Risks in the Anthropocene (C-CIA), CH-1205 Geneva, Switzerland*
[c] *Université Grenoble Alpes, Université Savoie Mont Blanc, CNRS, EDYTEM, 73000, Chambéry, France*
[d] *University of Dayton, Department of Geology and Environmental Geosciences, Dayton, OH, USA*
[e] *Institute of Fundamental and Applied Sciences, Duy Tan University, Ho Chi Minh City 700000, Vietnam*
[f] *Universidad Nacional Autónoma de México, Facultad de Filosofía y Letras, Ciudad Universitaria, Ciudad de México, 04510, Mexico*
[g] *Universidad de Playa Ancha, Facultad de Ciencias Naturales y Exactas, Departamento de Ciencias Geográficas, Laboratorio de Teledetección Ambiental (TeleAmb), Chile*
[h] *Adam Mickiewicz University, Institute of Geoecology and Geoinformation, Poznań, Poland*
[i] *Autoridad Nacional del Agua, Área de Evaluación de Glaciares y Lagunas, Huaráz, Peru*
[j] *Department of Geography University of Zurich, 8057 Zürich, Switzerland*
[k] *Faculty of Information Technology, Duy Tan University, Da Nang 550000, Vietnam*

A R T I C L E I N F O

Keywords:
Glacier retreat
Glacier extent reconstruction
Moraine mapping
Glacial lakes
Cordillera blanca

A B S T R A C T

In this study, we examine glacier retreat and associated processes in the Lejiamayu valley, central Cordillera Blanca, Peru (9.27°S; 77.48°W) since the Last Glacial Maximum (LGM). Based on detailed mapping of well-preserved moraines, we reconstruct glacier extent during the LGM, the Antarctic Cold Reversal (ACR) and the Little Ice Age (LIA), being 21.34 km^2 (LGM), 13.68 km^2 (ACR) and 6.84 km^2 (LIA). We document that glacier extent decreased to 2,86 km^2 since the end of the LIA in this catchment (ice loss 58%). In addition, we explore the colonization and growth of lichens and Schmidt-hammer rock test R-values over the deglaciated surfaces, suggesting a relationship to possible evironmental controls rather than to the timing of the exposure. Further, we use empirical glacier velocity-based equation to estimate maximum potential future volume of the new glacial lake forming in the upper part of the valley (4725 m a.s.l.; 2.2 Mm^3). We conclude that previous estimates of future lake volume might have been underestimated and that the sufficiency of the glacial lake outburst flood (GLOF) mitigation measures implemented at downstream located Lake Lejiacocha (4628 m a.s.l.) should be revised in future.

1. Introduction

Climate change-induced glacier decline affects high mountain regions all over the globe (IPCC, 2019; Zemp et al., 2019), impacting both natural as well as socio-economical systems in wider downstream-located areas (e.g. Huss et al., 2017; Brighenti et al., 2019; Immerzeel et al., 2020). These effects are particularly observable in the most glacierized tropical mountain range of the world - the Cordillera Blanca in Peru (Vuille et al., 2008; Schoolmeester et al., 2018; Vuille et al., 2018). This area has been a subject of numerous studies focusing on climate drivers, dynamics and consequences of glacier retreat since the Little Ice Age (LIA; e.g. Rabatel et al., 2013; Huh et al., 2017; Huh et al., 2018; Muñoz et al., 2020). Further, imprint of late Quaternary glaciations is rich in this area, with moraine record spanning from a multi-phased LIA back to at least MIS 10 (Farber et al., 2005; Solomina et al., 2007; Glasser et al., 2009; Smith and Rodbell, 2010; Giraldez, 2011; Mark et al., 2017; Hall et al., 2018).

Parts of the mountainous areas of the Cordillera Blanca which are located between the Last Glacial Maximum (LGM) limits and the current glaciers have undergone significant changes during the Holocene and have accommodated dynamic geomorphological processes. Notably, glacier-covered areas turned into the bare surfaces with massive

* Corresponding author.
E-mail addresses: aemmer@seznam.cz, adam.emmer@uni-graz.at (A. Emmer).

https://doi.org/10.1016/j.jsames.2021.103254
Received 7 November 2020; Received in revised form 12 February 2021; Accepted 22 February 2021
Available online 1 March 2021

moraine walls, overdeepened depressions filled with glacial lakes and unstable slopes. Being characterised by high process dynamics, numerous far-reaching process chains, such as destructive lake outburst floods (see Emmer, 2017) and slope movements (Klimeš et al., 2016), have been documented to be initiated in these areas.

Despite the efforts and progress in our understanding to glacier retreat-driven process chains, dynamics of these changes and associated hazards have been rarely explored on a detailed scale of individual valley. Using the example of the Lejiamayu valley, the main obectives of this study are: (i) to reconstruct the LGM, ACR and LIA glacier extent, based on geomorphological field evidence and moraine mapping; (ii) to reveal the controls of Schmidt-hammer rock test R-values and lichen growth (environmental controls, timing of the exposure) (iii) to estimate potential volume of a new glacial lake forming in the upper part of the valley and discuss its hazardousness in relation to the remedial works implemented downstream in 1950s.

2. Study Area: The Cordillera Blanca and the Lejiamayu valley

The Cordillera Blanca (8°-10°S; 77–78°W; see Fig. 1A), located in the Western Cordillera (Cordillera Occidental), is the highest Peruvian mountain range with numerous peaks towering above 6000 m a.s.l. (Huascarán Sur 6768 m a.s.l.). It hosts the largest portion of the world's tropical glaciers, with current extent being estimated less than 500 km^2 (Georges, 2004; Racoviteanu et al., 2008; Silverio; Jacquet, 2017; Veettil, 2018). The main ridge of the Cordillera Blanca is oriented in a NNW-SSE direction (parallel to the Pacific seashore) and divides the mountain range into the wetter eastern part drained by the Marañon River into the Atlantic Ocean while drier western part is drained by the Santa and Pativilca Rivers into the Pacific Ocean.

The Lejiamayu valley (Fig. 1B) is located on south west-facing slopes of the Nevado Copa (9°16'10"S; 77°28'52"W; 6188 m a.s.l.) – one of the six-thousanders located in the central part of the Cordillera Blanca - and is drained by the Río Lejiamayu river, which confluences with the Río

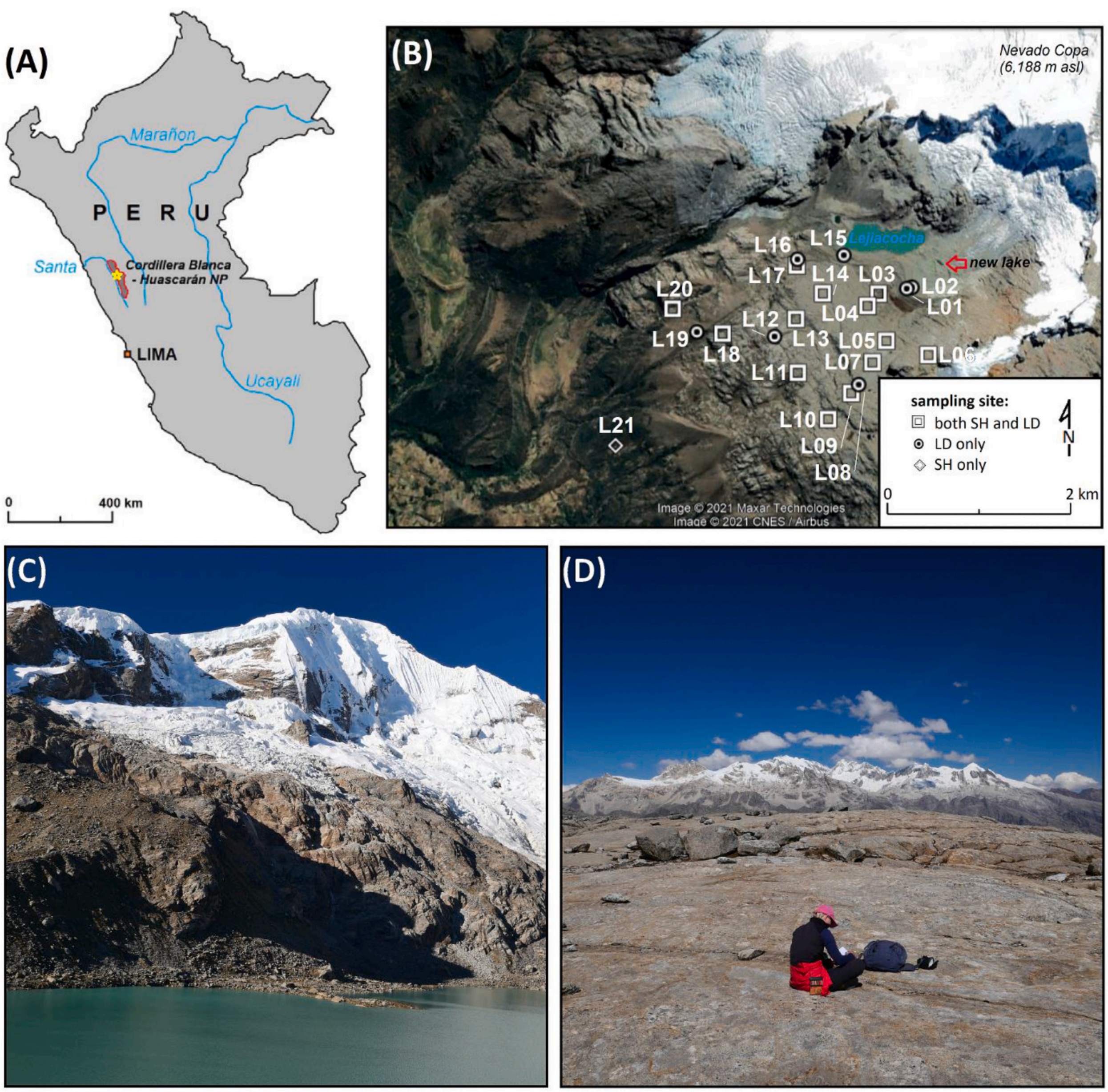

Fig. 1. The study area and the location of sampling sites. (A) Location of the Lejiamayu valley in the Cordillera Blanca (yellow star); (B) Location of lichenometric dating sites (LD) and Schmidt-hammer (SH) sampling sites in the Lejiamayu valley; (C) Lake Lejiacocha as seen from the left lateral moraine with Nevado Copa (6188 m a.s.l.) in the background; (D) An example of bedrock outcrop sampling site L10 with Nevado Tocllaraju (6032 m a.s.l.) in the background.

Alanquey river (3200 m a.s.l.) and then the Río Marcará river in Chancos (2865 m a.s.l.). The vertical difference of the Lejiamayu valley therefore reaches almost 3 km while it covers the area of approximately 18.5 km^2. According to the geological map of Peru 1:1,000,000 (IGM, 1975), the Lejiamayu valley is mainly formed by plutonitic granite and granite-diorite rocks which belong to the Cordillera Blanca batholit (see also Atherton and Sanderson, 1987), which are covered by marine facies of cretaceous age in the lower part of the valley. Visible sedimentary deposits associated with fluvial, glacio-fluvial and glacial activity are of quaternary age (ELECTROPERU, 1974). The upper parts of the catchment (above 4500–5000 m a.s.l.) are currently occupied by glaciers.

One large lake (Lejiacocha) and several small lakes are located in the valley. All these lakes are of glacial origin and according to the previous studies do not represent a threat of glacial lake outburst flood (GLOF; see Veliz et al., 1975; Emmer et al., 2016). Lake Lejiacocha (Fig. 1C) is dammed by massive moraine wall, has the surface area of 183,907 m^2 and a volume of 1,356,124 m^3 (INRENA, 2005; Muñoz et al., 2020). Lake Lejiacocha is equipped with dam remedial works - artificial outlet combining concrete outflow (open cut) with artificial dam built already in 1950s (Reynolds Geo-Sciences, 2003), keeping the lake level at 4618 m a.s.l. and providing a freeboard of 5 m.

3. Data and methods

3.1. Data

3.1.1. Field data

Field survey in the Lejiamayu valley took place in June 2019. Geomorphological mapping, lichenometric dating (LD) and Schmidt-hammer rock test (SH) were employed (see Fig. 1B and D). Our samplig strategy aimed at collecting samples throughout the surfaces deglaciated since the LGM (see locations in Fig. 1B), however it also reflects suitability for sampling (see description of individual methods) and terrain accessibility. LD was employed at moraines sites as well as on exposed bedrock outcrops (20 sampling sites; see 3.2.2) and SH was only used as a deglaciation relative dating tool on exposed bedrock outcrops (not applied on moraines; 14 sampling sites; see 3.2.1).

3.1.2. Remotely-sensed data

Both aerial and satellite images were employed to: (i) reconstruct post-LGM glacier extent over time, based on mapping of moraines supported by lichenometric dating. We used aerial images form the archive of the Autoridad Nacional del Agua in Huaráz (from 1948), Landsat images covering the study area since late 1970s (USGS, 2019) and high resolution USGS/CNES/Airbus images available via Google Earth Pro (Google LLC., 2019), covering the study area since 2003 (lower part of the valley)/2011 (upper part of the valley; see Table 1). For glacier surface velocity and ice thickness calculation, we employed two LANDSAT 8 (Band 8) scenes for the dates July 17, 2018 and July 19, 2019. ALOS PULSAR digital elevation model (DEM) of 12.5 m spatial resolution is used to extract topographic parameters. The modified RGI (v 6) glacier boundaries has been used for glacier delineation.

3.2. Methods

3.2.1. Schmidt-hammer rock test (SH)

SH method assumes that lately exposed surfaces have higher R-values (Rebound values) compared to surfaces exposed previously, due to the different duration of weathering. Employing SH rock test method requires petrological and geological uniformity of surveyed rock materials as well as the uniformity of orientation and inclination of measured surfaces. All these assumptions are met in the study area of the Lejiamayu valley, where horizontally oriented surfaces of granite-diorite have been surveyed. We used SH measurement device Proceq (N/NR type) with impact energy 2207 Nm and dimensionless scale 1–100 (Rebound values, R-values). This device has been calibrated by Technical and test institute for construction Prague, SOE (www.tzus.cz/en), a certified calibration branch office of Proceq.

SH measurements were performed at 14 sites (see Fig. 1B) and each site comprises of 25 individual measurements (measured R-values). Excluding 5 most extreme values (the most far from the average), 20 measurements were used for calculating R-value of the site (minimum, maximum, average, standard deviation), following the procedure suggested by Moon (1984). This method has been widely used previously (e.g. Haeberli et al., 2003; Goudie, 2006), because it presents a simple, easy-to-use dating approach which can be employed in remote high mountain areas. Using the example of the Churup valley located approximately 25 km to the south from the studied Lejiamayu valley, Emmer et al. (2019) have shown that SH can reliably distinguish between recently (i.e. post-LIA) and previously (i.e. post-LGM) deglaciated surfaces. However, the ability to distinguish the timing of deglaciation on the finer time scale was not proved. Therefore, we aim at employing SH for distinguishing the timing of deglaciation on centennial to millennial scale (surfaces deglaciated since the LGM).

3.2.2. Lichenometical dating (LD)

LD was employed to estimate the ages of moraine stabilisation and glacier retreat over the bedrock outcrops. The fundamentals of lichenometry for dating landforms have been laid down and experienced boom since 1970s and early 1980s (Osborn and Taylor, 1975; Gellatly, 1982; Innes, 1983, 1985). Numerous researchers adopted this method for dating moraines and deglaciated surfaces in Peru (e.g. Rodbell, 1992; Solomina et al., 2007; Forget et al., 2008; Jomelli et al., 2008; Emmer, 2017; Emmer et al., 2019), elsewhere in South America (Winchester and Harrison, 2000; Winchester et al., 2001; Harrison et al., 2007; Rabatel et al., 2008; Jomelli et al., 2009) as well as other regions across the globe (e.g. McCarroll, 1991; Solomina and Calkin, 2003; Matthews, 2005; Decaulne, 2016).

In our study, a total of 7 moraine deposits and 13 bedrock outcrops (see Fig. 1B) have been dated using LD, using the growth curves

Table 1
Overview of remotely-sensed images used in this study.

Sensor (provider)	Date of acquisition	Resolution	Scene/product ID
Aerial images	01-Sep-1948	2 m	1948_535, 1948_536, 1948_537, 1948_811, 1948_812, 1948_813
Landsat MSS	04-Aug-1975	60 m	LM02_L1TP_008066_19750804_20180426_01_T2
Landsat TM	21-Aug-1988	30 m	LT05_L1TP_008066_19880821_20170206_01_T1
	02-Sep-1998	30 m	LT05_L1TP_008066_19980902_20161222_01_T1
	18-Aug-2010	30 m	LT05_L1TP_008066_20100818_20161014_01_T1
USGS/Maxar Technologies	11-Jul-2003	<2m	NA[a]
Maxar Technologies	31-May-2011	<2m	NA[a]
CNES/Airbus	22-Jun-2019	<2m	NA[a]
Landsat OLI	17-Jul-2018	30 m	LC08_L1TP_008066_20180707_20180717_01_T1
	10-Jul-2019	30 m	LC08_L1TP_008066_20190710_20190719_01_T1
	19-Jul-2019	30 m	LC08_L1TP_008066_20190710_20190719_01_T1
ALOS PALSAR DEM	2015	12.5 m	Scene ID-AP_27249_FBS_F7000_RT1

[a] Google Earth Pro does not specify scene/product ID.

developed specifically for the western part of the Cordillera Blanca by Solomina et al. (2007) and Jomelli et al. (2008). Based on the methodological criteria defined by Solomina et al. (2007) and Jomelli et al. (2008), we performed the following procedure: (i) measuring living, circle-shaped individuals of *Rhizocarpon geographicum*; (ii) only the largest individual from each boulder is measured and boulders with diameters > 0.5 m are considered (this rule only applies for bouldery accummulations, i.e. moraines, not for bedrock outcrops, where largest individuals were searched in circle-shaped area with diameter of about 10 m); (iii) measuring 100 lichens at each sampling site.

Lichens were measured with a digital calliper that provides an effective measuring range of 0–100 mm and measurement accuracy of ± 0.005 mm was used for the measurement. Five largest lichens from each site were considered for age estimation, where relevant. Relict (dead) lichens were measured in order to determine an approximate minimum age of surface exposure/moraine deposition. In such a case, relict lichens with diameter >60 mm were considered indicating the age >1500 years, further refinement of this approximation and the extrapolation of the lichen growth curve is not reliable (see Osborn et al., 2015; Rosenwinkel et al., 2015; Decaulne, 2016). Due to the apparent limitations for estimating precise time of deglaciation, i.e. absolute dating (Osborn et al., 2015; Rosenwinkel et al., 2015; Emmer et al., 2019), we mainly used lichenometry for relative dating and differentiating LIA phases (see 4.1.2.) and as a complimetary information to glacio-geomorphological mapping.

3.2.3. Reconstructing Lejiamayu past glacier extent

Combining field survey and remotely sensed images, we exhaustively mapped moraine ridges throughout the Lejiamayu valley, spanning the elevation range from 3350 m a.s.l. (the lowermost part of the LGM moraines) to 4985 m a.s.l. (upper reaches of the LIA moraines; see Fig. 2). Following thorough mapping, individual moraines ridges were grouped as ‚stadials‘ representing significant former glacier positions based on morphological criteria (e.g. Schoeneich, 1998). We used the ‚superposition principle‘ in relative chronology of moraines (i.e. considering a sequence of moraines, those located at lower elevation are considered older). In a second step, we compared our local chronology to a synthetic regional chronostratigraphy to propose approximate dating for these features. Based on the recent literature of ^{10}Be-based moraine chronologies in the tropical Andes (Hall et al., 2009, 2018; Smith and Rodbell, 2010; Jomelli et al., 2014; Bromley et al., 2016; Stansell et al., 2017; Hall et al., 2018; Úbeda et al., 2019), we have distinguished between LGM moraines (Fig. 2A,B,C), early Lateglacial moraines (Fig. 2A), Antarctic Cold Reversal (ACR) moraines (Fig. 2D) and LIA moraines (first and the second phase; Fig. 2E and F). Early Holocene and Neoglacial positions have been suggested as well, but are nevertheless more difficult to distinguish from ACR and LIA moraines, respectively, based solely on relative dating criteria. Finally, glacier Equilibrium Line Altitude (ELA) for the reconstructed past stadials were derived from the geomorphological mapping. Maximum elevation of the upper bound of lateral moraines (so-called ‚MELM‘ method) is a robust surrogate for ELA elevation (Benn et al., 2005), as evidenced by previous works in the tropical Andes (Seltzer, 1992; Taggart, 2009).

3.2.4. Estimating potential future volume of new glacial lake

A supra-glacial lake has started forming just upstream of the Lejiacocha lake (Fig. 1B). The future expansion of the lake depends on the glacier bed topography and future glacier retreat. To calculate the future (maximum) extent and volume of the newly forming lake, initially the glacier bed is mapped using a spatially distributed ice-thickness approach (Linsbauer et al., 2012; Sattar et al., 2019; Magnin et al., 2020). The depressions present on the glacier bedrock (overdeepening), are identified as the potential lake formation sites in the future. In Peruvian Andes this approach has been previously employed to identify the future lakes in glaciated basins (Haeberli et al., 2016; Colonia et al., 2017). Here, laminar flow modeling based on glacier surface velocity, slope, and basal shear stress is performed to calculate the spatially distributed ice-thickness of the Lejiamayu glacier followed by the mapping of glacier-bed to calculate the extent of the overdeepening present at the glacier terminus. Shear-stress based methods to reconstruct glacier ice thickness (Linsbauer et al., 2012) is used. The relationship can be given as:

$$\tau_b = f\ \rho g H\ \sin\alpha \tag{1}$$

Where τ_b is the basal stress, H is the ice thickness, $\sin(\alpha)$ is the slope, ρ is the ice density, g is the acceleration due to gravity (9.8 ms^{-1}), f is the shape factor, which is defined as the ratio between the driving stress and basal stress along a glacier (Gantayat et al., 2014) and has a range of 0.6–1.0. As basal stress measurements are not easily available for many glaciers in Peruvian Andes (including Lejiamayu glacier) we use glacier surface velocity to calculate the ice thickness (H). The relation is empirically given by:

$$U_s = U_b + \frac{2F}{n+1}(\tau_b)^n H \tag{2}$$

Where U_s is the surface velocity (ms^{-1}), U_b is the basal velocity which is assumed to be 25% of Us (Gantayat et al., 2014), F is the creep parameter which is assigned a constant value of 3.24×10^{-24} $Pa^{-3}s^{-1}$ for temperate glaciers (Cuffey and Paterson, 2010), n is Glen's flow constant with a value assumed to be 3, τ_b is the basal stress, and H is the ice thickness (in m).

Combining equations (1) and (2), glacier ice-thickness (H) can be calculated by:

$$H = \sqrt[4]{\frac{1.5\ Us}{F\ (f\rho g sin\alpha)^3}} \tag{3}$$

In the above equation, glacier-surface velocity (U_s) is derived using a sub-pixel correlation method using two optical satellite images (see Section 3.1.2 for data used) temporally separated by one year (Scherler et al., 2008). As LANDSAT 8 provides a co-registered and correlated panchromatic band with a spatial resolution of 15 m, the displacement measurements are more accurate and are comparable to field measurements (Sattar et al., 2019). Sattar et al. (2019) justified the accuracy of this image correlation technique to effectively estimate glacier velocity by comparing the displacement measurements obtained over the stable ground. Here the COSI-CORR (Co-registration of Optically Sensed Images and Correlation) module in ENVI image-processing software that performs image-to-image correlation at a sub-pixel level is used. The glacier ice thickness of the Lejiamayu glacier is calculated using Eq. (3). The glacier bed is further mapped based on GIS-based operation using glacier boundary (RGI v 6.0), spatially distributed ice thickness, and surface elevation (DEM). Previous studies compared glacier surface-velocity based ice-thickness with Ground penetrating radar (GPR) estimates to show the reliability of this approach to reconstruct glacier ice-thickness (Gantayat et al., 2014; Sattar et al., 2019). The future volume of the lake is compared to different area-based scaling methods.

4. Results

4.1. Post-LGM glacier variations in the Lejiamayu valley

4.1.1. Glacier stadials reconstruction

Our mapping covers the entire Lejiamayu catchment, both the trunk valley and a low gradient and glacially-sculpted bedrock area to the south (Fig. 3). Two well-preserved latero-frontal moraine ridges are present in the piedmont part of the Lejiamayu valley (see Fig. 2A). The most prominent outer ridges reach 3350 m a.s.l. and are considered as marking the LGM position. This is consistent with mapping effort conducted in the nearby Hualcán west massif, where Giraldez (2011)

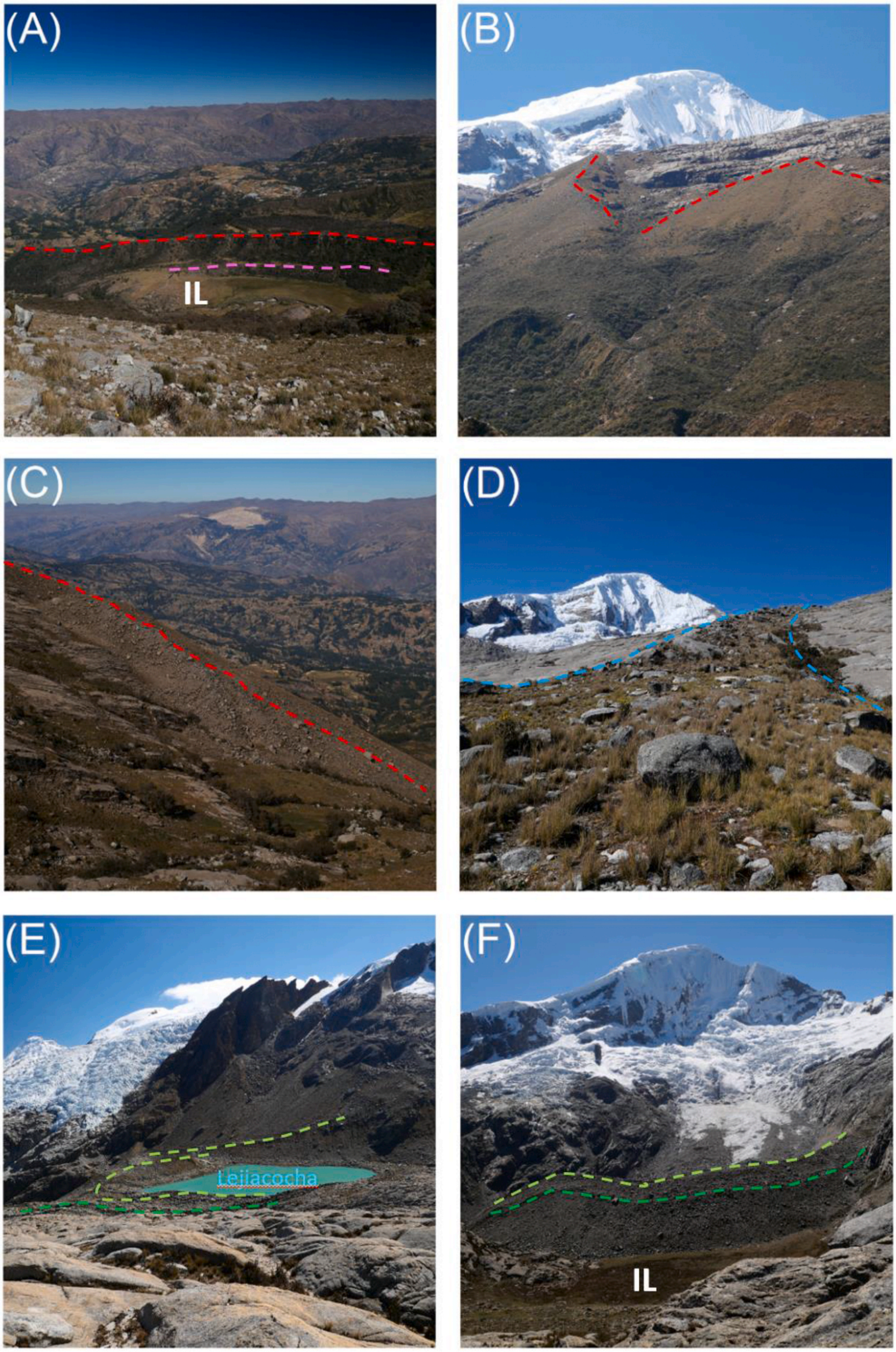

Fig. 2. Moraines of the Lejiamayu valley (marked with dashed lines, colors correspond to main mapped generations of moraines as used in Fig. 3). (A) LGM and Lateglacial moraines in the lower (piedmont) part of the Lejiamayu valley (3500–3,600m a.s.l.) with infilled lake (IL) visible in thecentral part of the image; (B) LGM moraines on slopes (4050–4300 m a.s.l.); (C) LGM moraine on slope (4100–4200 m a.s.l.); (D) ACR moraine (4500–4600 m a.s.l.); (E) LIA moraine damming Lake Lejiacocha (4600–4700 m a.s.l.); (F) Early Holocene and LIA moraine in the upper part of the valley (4700–4750 m a.s.l.) with infilled lake (IL) visible in the lower central part of the image in front of the moraine wall.

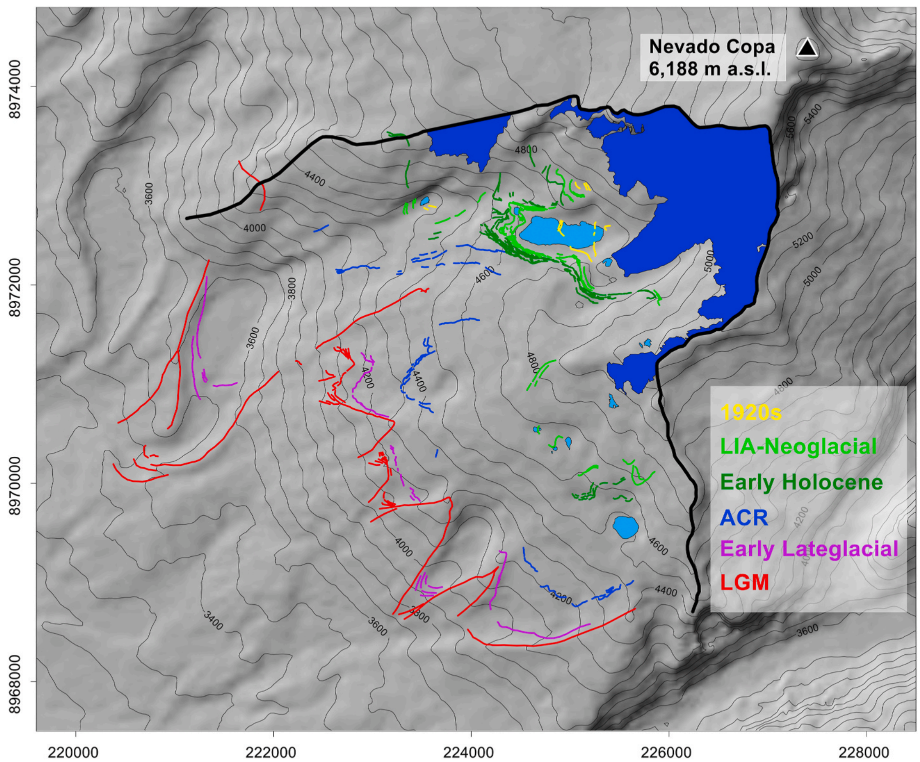

Fig. 3. Detailed glacio-geomorphologic map of the Lejiamayu valley. Moraines were attributed to six main generations based on morpho-stratigraphic relationship and correlation with regional chronostratigraphy (see Sections 4.1 and 5.1). Current glacier extent (2019) is shown. Grid UTM 18S in meters.

similarly traced those moraines down to 3350 m a.s.l. The uppermost bound of the large left lateral LGM moraine is detectable up to 4460 m a.s.l., which provide a first order estimate of the ELA for this stadial. This value is slightly higher than LGM ELA usually reported to be around 4300 m a.s.l. in CB (Mark et al., 2017). This could be due to the composite nature of this landform, whose upper part may have been deposited during an early lateglacial stadial.A set of less prominent but sharply crested inner ridges is present at 3490–3540 m a.s.l. in the trunk

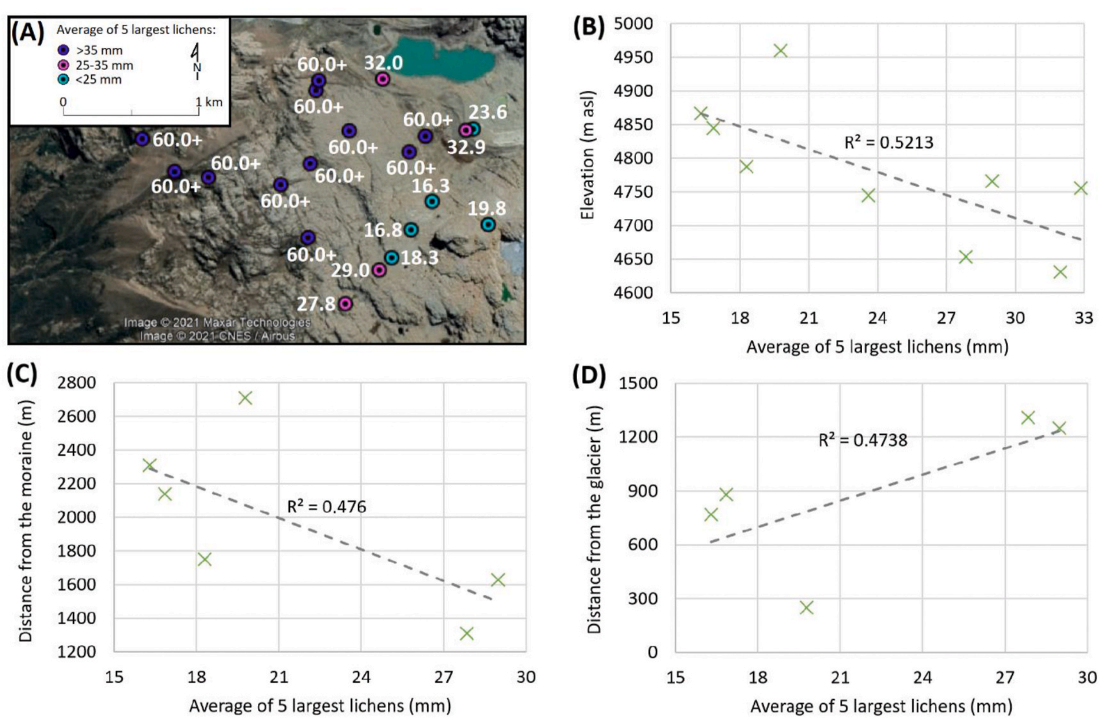

Fig. 4. Lichens and possible environmental controls of lichens' growth. (A) Location of individual sampling sites and average of 5 largest lichens found; (B) Relationship between the average of 5 largest lichens and elevation of sampling sites; (C) Relationship between the average of 5 largest lichens and distance from moraines; (D) Relationship between the average of 5 largest lichens and distance from current position of glaciers.

valley. Similarly, in the southern area, LGM moraines are accompained by nested inner early lateglacial moraines located just few hundred meters upstream (Fig. 3).

ACR moraines are more discontinuous and no frontal moraine has been preserved in the trunk valley owing to steep terrain. ACR front location has been estimated with reasonable precision to 4000 m a.s.l. based on latero frontal moraines. Highest ACR ridge remnants are observed up to 4640 m a.s.l. (see Fig. 2D) and provide reliable estimate for the ELA prevailing during this stadial. This is in good agreement with a mean AABR ELA of 4650 ± 200 m a.s.l. determined in the Hualcán west massif by Giraldez (2011), although this stadial was called Younger Dryas by this author. Given its size, the moraine complex dammimg Lejiacocha lake was build during numerous Holocene oscillations. Superimposed on this complex are Neoglacial ridges and at least two generations of freshly looking LIA ridges (see Fig. 2E and F), with a LIA front at 4550 m a.s.l. LIA moraines can be traced up to 4985 m a.s.l., similar to the LIA AABR ELA values for the Hualcán west massif at 4995 ± 125 m a.s.l. (Giraldez, 2011).

4.1.2. Lichenometric dating

We found relict lichens >60 mm indicating possible age >1500 years at 11 sampling sites (see Fig. 3A), and datable lichens at 9 sampling sites (see Fig. 4A). LD over the exposed bedrock surfaces revealed that some of the recently deglaciated surfaces (L05 to L10) might have been glaciated during the LIA, despite these areas are not surrounded by well-visible moraines such as those found in the main valley. Two or three generations of LIA moraines are observable in the field (two clearly distinguishable lateral moraine ridges; see Fig. 2E and two frontal moraines, Fig. 3). The second moraine ridge (sampling site L01) has been dated to the mid-phase of the LIA (average of 5 largest lichens 32.6 mm; 365–405 years ago, i.e. 1615-1655 AD) as defined by Thompson et al. (2000) and Solomina et al. (2007), while the inner moraine ridge corresponds with the latest LIA (23.6 mm; 220–250 years ago, i.e. 1770-1800 AD). Lichens <20 mm were found at sampling sites L05 – L08. We plotted measured lichens against possible environmental controls of their occurrence (elevation, distance from downstream located moraines and distance from current position of glaciers). Fig. 5 shows that the average of the 5 largest lichens is decreasing with elevation and the distance from the LGM moraine and increasing with distance from the glacier.

4.1.3. The LGM, ACR, LIA and present-day glacier extent

Combining field and remotely sensed data-based mapping of moraines (see 4.1.1), we estimate a LGM glacier extent of 21.34 km^2, and a LIA glacier extent of 6.84 km^2. Despite some missing moraine imprints, we estimate an ACR glacier extent of 13.68 km^2 (see Fig. 5). Modern glacier (year 2019) occupies an area of 2.86 km^2, which implies a 58% of glacier loss since the LIA glacier maximum.

4.2. Schmidt-hammer rock test over deglaciated surfaces

SH has been employed at 14 sampling sites located between 3772 m a.s.l. (L21) and 4960 m a.s.l. (L06). All the sampling sites are located in the area which is thought to be glaciated during the LGM (see 4.1.1). The only exception is L21, which is bedrock outcrop located further downstream of the LGM moraine, i.e. in the area thought not to be glaciated in the past (tens of) thousands years. Measured average R-values varies from 55.1 (STDEV 3.6; sampling site L05) to 44.9 (STDEV 4.1)/35.2 (STDEV 5.3) at sampling sites L17/L21 (see Fig. 6A). Assuming possible LIA extent based on lichenometric dating (see 4.1.1), an average R-value of sampling sites located within the LIA limits is 49.4 (STDEV 5.0), while an average R-value of sampig sites located outside the LIA limits is 46.5 (STDEV 6.5), which does not really distinguish between these two zones.

To explore the relationship with selected environmental controls, we plotted measured SH values against the elevation of sampling sites (Fig. 6B), distance from the current position of glacier (Fig. 6C) and distance from downstream located LGM moraines (Fig. 6D). As for the relationship to the elevation of sampling sites, we observe increasing R-values with increasing elevation ($R^2 = 0.31$) and even more profound relationship when not considering outlier L20 ($R^2 = 0.71$). Furthermore,

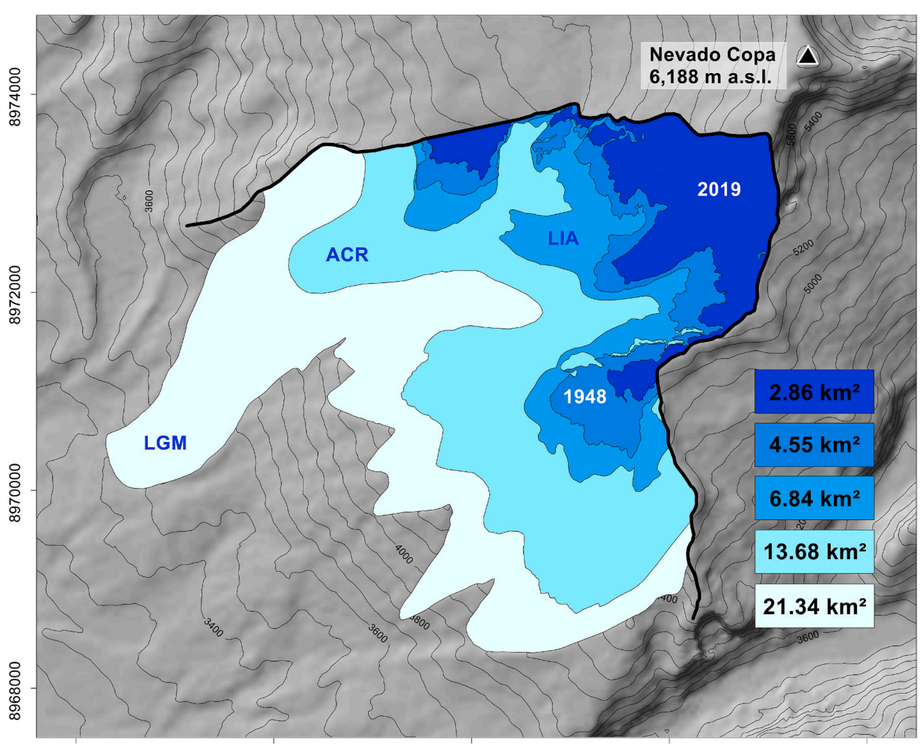

Fig. 5. Reconstruction of the Lejiamayu glacier extent for the LGM, ACR and LIA stadials based on the moraine record. The 1948 and 2009 glacier extent are also shown. Grid UTM 18S in meters.

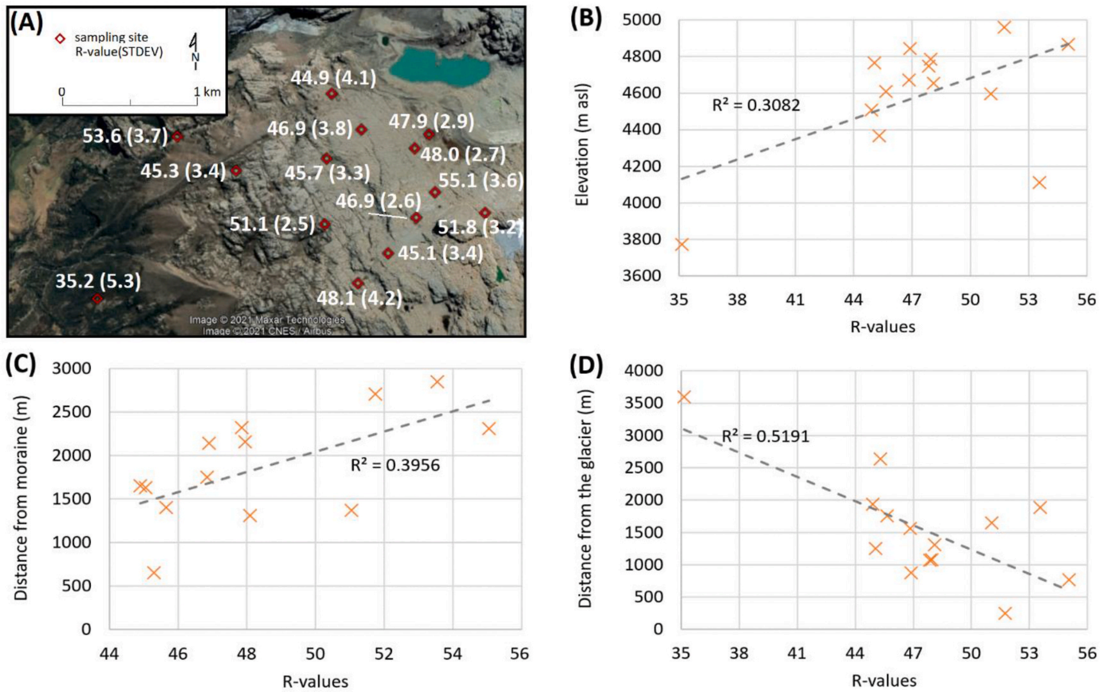

Fig. 6. Schmidt-hammer rock test and possible environmental controls. (A) Location of individual sampling sites and average R-values; (B) The relationship between R-values and elevation of sampling sites; (C) The relationship between R-values and distance from moraines; (D) The relationship between R-values and distance from current position of glaciers.

increasing trend in R-values with decreasing distance from the glacier is observed ($R^2 = 0.52$). By contrast, an increasing trend in R-values with increasing distance from LGM moraines is observed ($R^2 = 0.40$).

4.3. Maximum future extent of the new glacial lake

The surface velocity derived using the subpixel correlation technique is employed to determine the spatially distributed glacier ice thickness. The velocity measurements (Fig. 7A) reveal that the Lejiamayu glacier has a surface-flow speed of 0–7 ma^{-1} near the present terminus. The velocity varies between 7 and 28 ma^{-1} towards the upper part of the ablation zone. The glacier ice thickness calculated using Eq.(3) shows a ice-thickness of 0–27 m near the present terminus (Fig. 7B). The ice gradually thickens towards the upper ablation zone with ice-depths reaching up to 98–157 m. Furthur, GIS-based raster calculation (DEM minus Ice thickness distribution) revealed the spatially distributed glacier-bed topography. An overdeepening on the glacier bed is mapped that is present at the present terminus extending up to a distance of 720 m upstream. The maximum width of the overdeepening is 280 m and has a total area of 0.16 km^2. The spatially distributed depth of the over-deepened site shows a maximum depth of 43 m (Fig. 7C).

The depth gradually increases from the periphery towards the center of the overdeepening, where it is the maximum. It is seen that the newly forming supraglacial lakes lies at the frontal part of the glacier. As these small supraglacial lakes are located over the overdeepend site, it is likely that as the glacier melts/retreats the melt water would be trapped in the depression (overdeepening) and eventually grow to form a larger lake with a maximum extent as the overdeepened site. The total volume of the overdeeping based on the modeled ice thickness is calculated to be 2.20 x 10^6 m^3. This calculated volume is further compared to the different empirically calculated volumes (see Table 2). Muñoz et al. (2019) gave an empirical relationship based on lake width and total area to calculate the volume of the lakes in Cordillera Blanca, Peru. Here, we compare the modeled volume to the empirically calculated volume. It is seen that the modeled volume is in line with the empirical volume (Muñoz et al., 2019) with a difference of less than 1%. The volume calculated using the equation proposed by Evans (1986) represents a difference of 3.2%. The volumes calculated using the equations of Huggel et al. (2002) and Cook and Quincey (2015) show a difference of 15.0% and 20.8% respectively.

5. Discussion

5.1. Timing of post-LGM glacial evolution in the Lejiamayu valley

Detailed geomorphological mapping allow us to identify six main generations of moraines (Fig. 3). We now rely on existing evidence in CB to discuss the absolute timescale of their emplacement. The outermost moraine complex was deposited during the LLGM, dated in CB between ~40 and 25 ka, i.e. slightly earlier than MIS2 (Mark et al., 2017; Úbeda et al., 2019). Immediately inboard of the prominent LGM moraines (>50 m local relief), a set of well-defined smaller ridges is widespread. This ensemble should correspond to the first recurrences (or stillstands) post-dating full glacial conditions and dated to ~18.5 ka in CB (Farber et al., 2005; Glasser et al., 2009; Smith and Rodbell, 2010; Mark et al., 2017). The third stadial is reconstructed from discontinuous ridge remnants due to an unfavourable preservational setting (steep bedrock slabs) which did not allow the conservation of a frontal moraine. Morphometric data permit to assign this stadial to the ACR, as in the tropical Andes ACR moraines are generally found midway between LGM and LIA positions (e.g. Bromley et al., 2016, see their figures S3–S4). This multi-phased cold climate event (Jomelli et al., 2014, 2017; Martin et al., 2020) has reversed the Lateglacial warming trend between ~14.5 and 12.9 ka in the tropical Andes. In CB, related moraines were ^{10}Be dated around 14.2 to 13.8 ka (Farber et al., 2005; Glasser et al., 2009; Smith and Rodbell, 2010; Stansell et al., 2017; Hall et al., 2018).

The following Younger Dryas chronozone has been mostly a period of glacier retreat in CB (Rodbell and Seltzer, 2000). The attribution of the fourth moraine set to the early Holocene draw on substantial evidence for moraines dated to 11.5–9.5 ka and located immediately

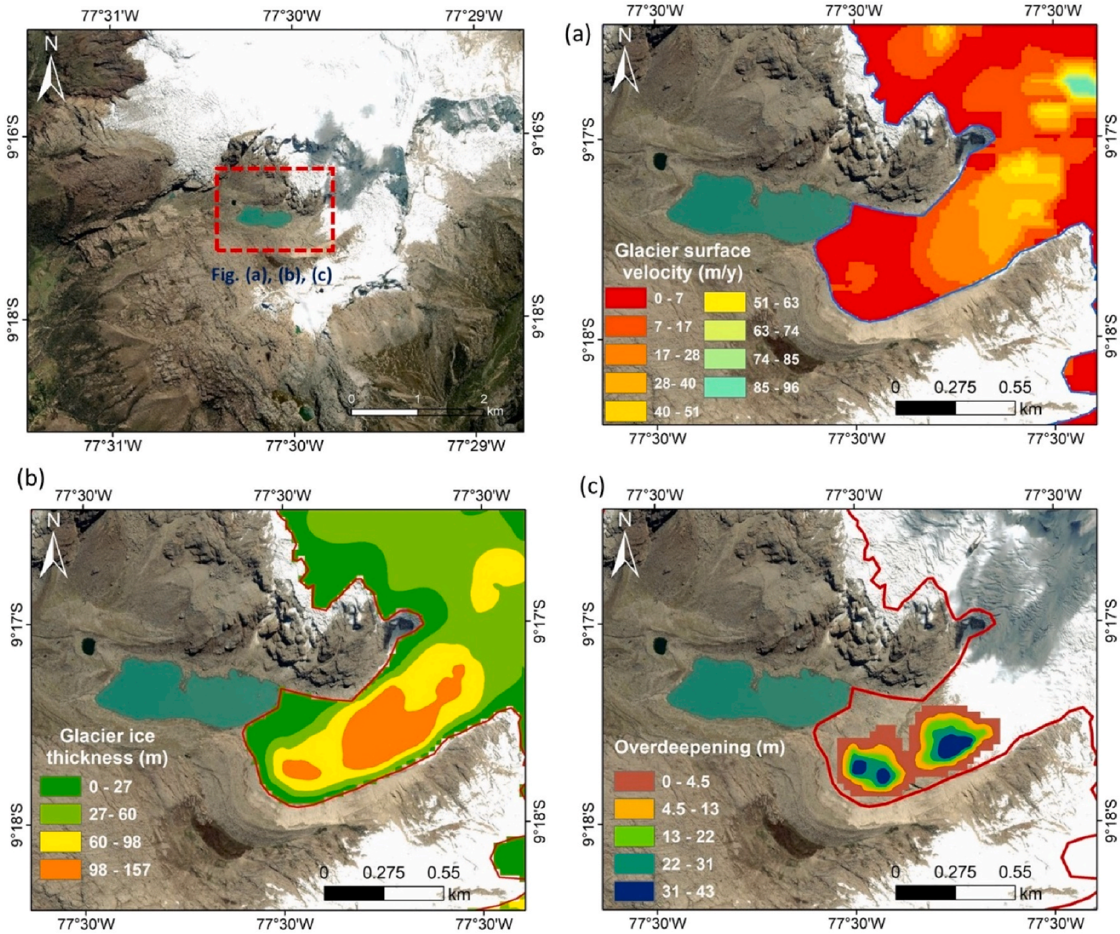

Fig. 7. Glacier bed overdeepening. (A) Glacier surface velocity of the Lejiamayu glacier; (B) Spatially distributed glacier ice thickness; (C) Spatially distributed depth of the overdeepened site on the glacier bed.

outboard of late Holocene moraines (e.g. Glasser et al., 2009; Stansell et al., 2017; Hall et al., 2018; Úbeda et al., 2019). At that time, Lejiacocha and former right-hand tributary Copa glacier southern diffluence were still confluent – before splitting somewhere between the mid Holocene and the onset of the late Holocene, a period of reduced glacier activity in the region (Stansell et al., 2017). Alternatively, some of the (innermost) moraines allocated to this period could correspond to the Neoglacial period, since Neoglacial deposits pre-dating the LIA are sometimes.dated in CB (Úbeda et al., 2019).The fifth moraine stadial encompasses the LIA. Three sub-sets of LIA moraine can tentatively be identified here. LD sampling sites lie on the two innermost (Fig. 3B) with results pointing to deposition during mid-to late-LIA. It shows that LIA maxima could have possibly been reached earlier than 17th century, likely around 0.7–0.6 ka (e.g. Jomelli et al., 2008; Emmer, 2017; Úbeda et al., 2019). Given the highly resolved and well-preserved moraine suite here, this could be a suitable site to refine the Holocene moraine stratigraphy in CB, if absolute ages could be acquired.

Less pronounced glacier advances were reported in the early 20th Century in CB (Georges, 2004). Mapped sixth moraine stadial is represented by a set of small ridges visible in the middle of the Lejiacocha lake (see Fig. 1C). These in-lake moraines were deposited during a glacier advance known to have occurred in the 1920s (Kinzl, 1942; Georges, 2004). Afterwards, a marked retreat caused lake final size to be reached following another still-stand with moraine deposition in the early 1950s (Fig. 3B). The post-LIA retreat of glaciers in the Lejiamayu valley and glacier ice loss of 58% is in agreement with observations from other glaciers in the Cordillera Blanca, exhibiting increased rate betwen 1990s and 2010s (e.g. Veettil 2018; Silverio and Jaquet, 2017) and other Cordilleras of Peru (e.g. López-Moreno et al., 2020). Even though there are descrepencies in the observed glacier surface changes in the Cordillera Blanca, which are arising from different data used or methodology adapted for processing satellite or aerial photographs. Nevertheless, the trend in glacier area is clearly decreasing over time and confirms a decline of tropical andean glaciers (Veettil and Kamp 2017).

5.2. Past, present and future glacial lakes and sufficiency of existing GLOF mitigation measures

Field data evidence that several lakes had existed and became extinct within the areas deglaciated since the LGM. Strikingly, the LGM and Lateglacial moraines located in the lowermost part of the valley likely retained a lake in the past (elevation 3550 m a.s.l.; see Fig. 3A), which

Table 2
Volume of the overdeepened site calculated using different approaches.

Volume estimation approach	Laminar flow approach (this study)	V1 = 0.104A^1.42 (Huggel et al., 2002)	V2 = 0.035A^1.5 (Evans 1986)	V3 = 0.1217A^1.4129 (Cook and Quincey, 2015)	V4 = A*Md_Wi (Muñoz et al., 2019)
Volume (x 10^6 m^3)	2.20	2.58	2.28	2.79	2.18

has been filled with sediments. The area of this lake might have exceeded 450,000 m^2, which is comparable to the largest lakes currently found in the Cordillera Blanca (Emmer et al., 2020). Apart from that, a moraine-dammed lake (25,000 m^2; 4715 m a.s.l.) was trapped in front of the Early Holocene moraine and the upper part of the valley (see Fig. 2F) and several smaller infilled bedrock-dammed lakes are observed in the overdeepenings all over the study area. No lake is mapped in the Lejiacocha valley by Kinzl and Schneider (1950), building on 1932 expedition.

Seven glacier-detached lakes (with area >2500 m^2) and one group of supraglacial lakes are currently (in 2019) located in the Lejiamayu valley, with the Lake Lejiacocha being the largest one. Since 1950s, the Lejiacocha Lake is equipped with the concrete artificial outlet and artificial dam providing a freeboard of 5 m (see Fig. 8). This type of mitigation measure was shown to be effective in mitigation glacial lake outburst floods (GLOFs) induced by slope movements into the lake/ floods from lake located upstream by preventing dam from overtopping and providing certain retention volume (Emmer et al., 2018). Concrete lake outflow also prevent erosion of the dam in case of increased discharge. Considering lake area 183,907 m^2 (INRENA, 2005), the retention volume calculated as a product of lake area and dam freeboard is about 920,000 m^3.

Guardamino et al. (2019) in their nation-wide study estimated that future lake upstream Lejiacocha could have a maximum length 302 m, maximum width 168 m and medium depth of 22 m, resulting in total volume of 612,000 m^3, suggesting that entire flood from this lake would be retained by Lejiacoca (not considering possible dam overtopping by displacement wave). Our results (upstream lake volume 2.20×10^6 m^3; see Table 2) however indicate that these numbers might be underestimated, suggesting that GLOF hazard mitigation measures might not be sufficient in future if the new lake reaches predicted size and burst out.

6. Conclusions

The Lejiamayu valley experienced extensive glacier ice loss since the

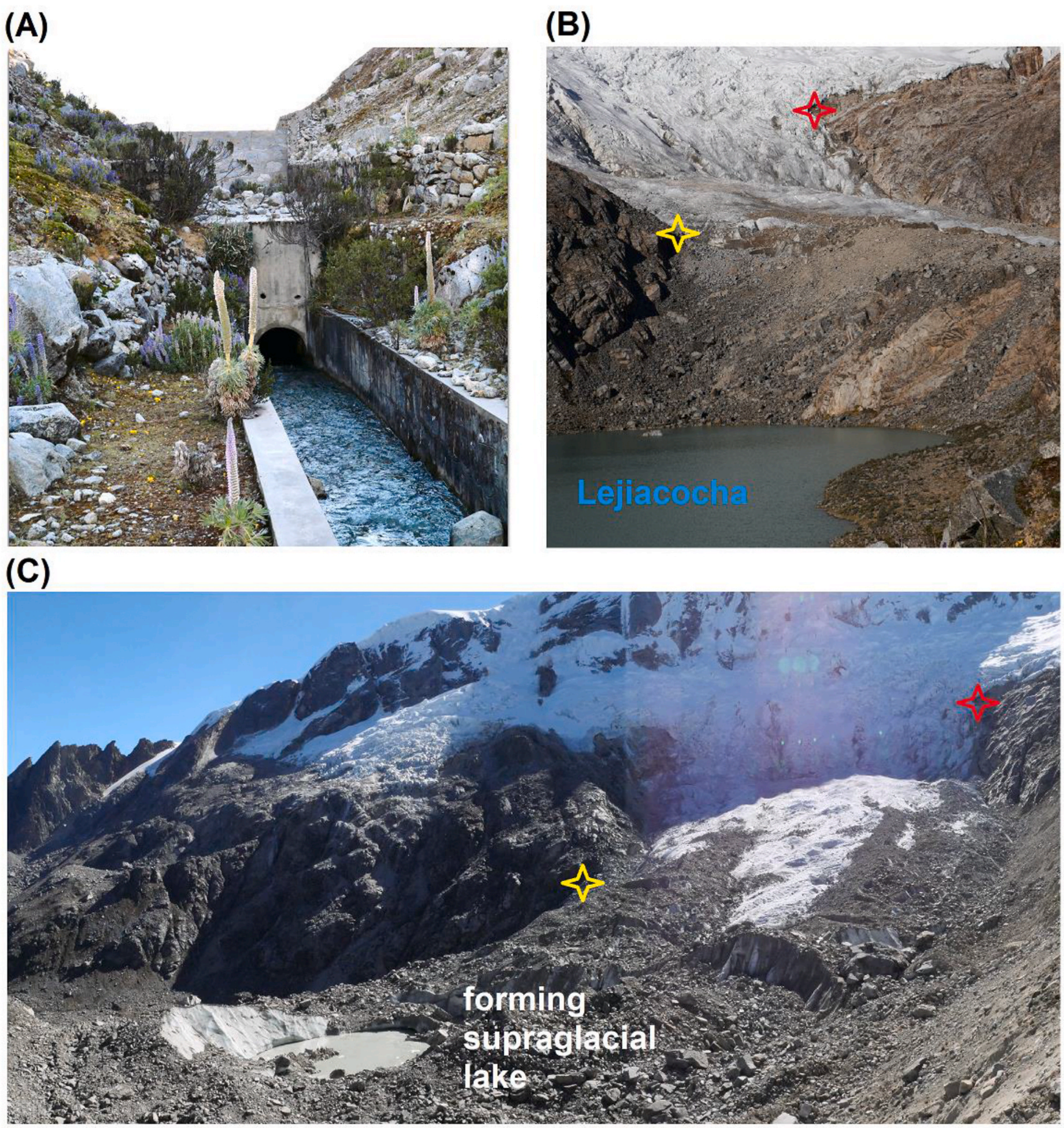

Fig. 8. GLOF hazard mitigation measures at the Lejiacocha lake and new lake forming upstream. Part (A) shows GLOF mitigation measure implemented at the dam of Lake Lejiacocha, providing 5 m freeboard; part (B) shows upstream view on the glacier snout on which supraglacial lake is located currently (in 2019); part (C) shows glacier snout located upstreal Lake Lejiacocha with forming supraglacial lake (lake area approximately 5000 m^2 in 2019). Yellow and red stars on (B) and (C) indicate identical locations on both images.

LGM, exposing approximately 20 km^2 of bare surfaces. We integrated field, documentary and remotely sensed data in order to provide some insights into the history, present and also the future of glaciation in this valley. A well-preserved moraine record allowed us to reconstruct LGM (21.34 km^2), ACR (13.68 km^2) and LIA (6.84 km^2) glacier extents. The post-LIA glacier retreat reduced the LIA glacier extene by 58% by 2019, leaving behind brand new landscapes. By employing Schmidt-hammer rock test, we explore how exposed bedrock surfaces react to the timing of deglaciation, showing only limited ability to distinguish between individual stages of the glaciation, but rather a relationship to related environmental controls (elevation, distance from the glacier and the moraine). Further, we focused our attention to the formation of a new glacial lake in the upper part of the valley and calculated its potential future volume. We conclude that the new lake will form behind the rock step upstream the LIA moraine-dammed Lake Lejiacocha and we argue that this new lake might reach larger volumes (2.2 Mm^3) than estimated previously, suggesting possible insufficiency of existing lake outburst flood mitigation measures.

Authors contributions

AE designed the study, collected, analysed and interpreted field data, MLR mapped moraines and reconstructed past glacier extents, BKV analysed dynamics of glacier retreat and AS modeled maximum future volume of new glacial lake. JRA, NC, and JM interpreted remotely sensed images. AC provided lake bathymetry map and documentary data from the archive of Autoridad Nacional del Agua in Huaráz. All authors contributed to the writing process and approved the final version of the manuscript.

Declaration of competing interest

The authors declare that they have no known competing financial interests or personal relationships that could have appeared to influence the work reported in this paper.

Acknowledgement

We thank anonymous reviewer for insightful comments and suggestions which helped to improve initial version of this study. AE acknowledge the financial support by the University of Graz. AE is a member of the RCUK-CONICYT Glacial Lakes of Peru (GLOP) project. AS is supported by the "Swiss Government Excellence Postdoc Award". We thank Sarah Hall and Jose Ubeda for sharing unpublished ^{10}Be dating results and for fruitful discussions about late Quaternary glacier variations in CB. This paper was developed in the frame of activities of ARNEES community (Alpine Research Network of Early carEer Scientists).

References

Atherton, M.P., Sanderson, L.M., 1987. The Cordillera Blanca Batholith – a study of granite intrusions and the relation of crustal thickening to peraluminosity. Geol. Rundsch. 76 (1), 213–232.

Benn, D.I., Owen, L.A., Osmaston, H.A., Seltzer, G.O., Porter, S.C., Mark, B.G., 2005. Reconstruction of equilibrium-line altitudes for tropical and sub-tropical glaciers. Quat. Int. 138–139, 8–21.

Brighenti, S., Tolotti, M., Bruno, M.C., Wharton, G., Pusch, M.T., Bertoldi, W., 2019. Ecosystem shifts in Alpine streams under glacier retreat and rock glacier thaw: a review. Sci. Total Environ. 675, 542–559.

Bromley, G.R.M., Schaefer, J.M., Hall, B.L., Rademaker, K.M., Putnam, A.E., Todd, C.E., Hegland, M., Winckler, G., Jackson, M.S., Strand, P.D., 2016. A cosmogenic ^{10}Be chronology for the local last glacial maximum and termination in the Cordillera Oriental, southern Peruvian Andes: implications for the tropical role in global climate. Quat. Sci. Rev. 148, 54–67.

Colonia, D., Torres, J., Haeberli, W., Schauwecker, S., Braendle, E., Giraldez, C., Cochachin, A., 2017. Compiling an inventory of glacier-bed overdeepenings and potential new lakes in de-glaciating areas of the Peruvian Andes: approach, first results, and perspectives for adaptation to climate change. Water 9, 336.

Cook, S.J., Quincey, D.J., 2015. Estimating the volume of Alpine glacial lakes. Earth Surface Dynamics 3, 559–575.

Cuffey, K.M., Paterson, W.S.B.(, 2010. The Physics of Glaciers. Academic Press, Cambridge, MA.

Decaulne, A., 2016. Lichenometry in Iceland, results and application. Géomorphol. Relief, Process. Environ. 22 (1), 77–91.

ELECTROPERU, 1974. Laguna Lejiacocha – Plano Geologico 1:2,000. ELECTROPERU, 1p.

Emmer, A., 2017. Geomorphologically effective floods from moraine-dammed lakes in the Cordillera Blanca, Peru. Quat. Sci. Rev. 177, 220–234.

Emmer, A., Klimeš, J., Mergili, M., Vilímek, V., Cochachin, A., 2016. 882 lakes of the Cordillera Blanca: an inventory, classification, evolution and assessment of susceptibility to outburst floods. Catena 147, 269–279.

Emmer, A., Vilímek, V., Zapata, M.L., 2018. Hazard mitigation of glacial lake outburst floods in the Cordillera Blanca (Peru): the effectiveness of remedial works. Journal of Flood Risk Management 11 (S1), 489–501.

Emmer, A., Juřicová, A., Veettil, B.K., 2019. Glacier retreat, rock weathering and the growth of lichens in the Churup Valley, Peruvian Tropical Andes. J. Mt. Sci. 16 (7), 1485–1499.

Emmer, A., Harrison, S., Mergili, M., Allen, S., Frey, H., Huggel, C., 2020. 70 years of lake evolution and glacial lake outburst floods in the Cordillera Blanca (Peru) and implications for the future. Geomorphology 365, 107178.

Evans, S.G., 1986. The maximum discharge of outburst floods caused by the breaching of man-made and natural dams. Can. Geotech. J. 23 (3), 385–387.

Farber, D.L., Hancock, G.S., Finkel, R.C., Rodbell, D.T., 2005. The age and extent of tropical alpine glaciation in the Cordillera Blanca, Peru. J. Quat. Sci. 20 (7–8), 759–776.

Forget, M.E., Thouret, J.C., Kuentz, A., Fontugne, M., 2008. Inherited glacial and periglacial landforms, and recent evolution of the Nevado Coropuna in the Central Andes of southern Peru. Géomorphol. Relief, Process. Environ. 2, 113–132.

Gantayat, P., Kulkarni, A.V., Srinivasan, J., 2014. Estimation of ice thickness using surface velocities and slope: case study at Gangotri Glacier, India. J. Glaciol. 60, 277–282.

Gellatly, A.F., 1982. Lichenometry as a relative-age dating method in mount Cook national part, New Zealand. N. Z. J. Bot. 20 (4), 343–353.

Georges, C., 2004. 20th-Century glacier fluctuations in the tropical Cordillera Blanca. Perú, Arctic, Antarctic, and Alpine Research 36 (1), 100–107.

Giraldez, C.M., 2011. Master thesis. Glacier Evolution in the South West Slope of Nevado Hualcán (Cordillera Blanca, Perú), vol. 59p. Complutense University of Madrid.

Glasser, N.F., Clemmens, S., Schnabel, C., Fenton, C.R., McHargue, L., 2009. Tropical glacier fluctuations in the Cordillera Blanca, Peru between 12.5 and 7.6 ka from cosmogenic Be-10 dating. Quat. Sci. Rev. 28 (27–28), 3448–3458.

Google, L.L.C., 2019. Google Earth Pro 7.

Goudie, A.S., 2006. The Schmidt Hammer in geomorphological research. Prog. Phys. Geogr. 30 (6), 703–718.

Guardamino, L., Haeberli, W., Muñoz, R., Drenkhan, F., Tacsi, A., Cochachin, A., 2019. Proyección de Lagunas Futuras en las Cordilleras Glaciares del Perú. Autoridad Nacional del Agua, Lima, Peru, p. 63p.

Haeberli, W., Brandová, D., Burga, C., Egli, M., Frauenfelder, R., Kääb, A., Maisch, M., 2003. Methods for absolute and relative age dating of rock-glacier surfaces in alpine permafrost. Permafrost. In: Phillips, M., et al. (Eds.), 1, pp. 343–348, 2.

Hall, S.R., Farber, D.L., Ramage, J.M., Rodbell, D.T., Finkel, R.C., Smith, J.A., Mark, B.G., Kassel, C., 2009. Geochronology of quaternary glaciations from the tropical Cordillera huayhuash, Peru. Quat. Sci. Rev. 28 (25–26), 2991–3009. https://doi.org/10.1016/j.quascirev.2009.08.004.

Hall, S.R., McKenzie, J.M., Hall, B.L., Meriaux, A.S.B., Fortin, M.A., 2018. Transecting the Cordillera Blanca of Northern Peru: a Glacial Geochronology Determined from ^{10}Be Exposure Ages of Moraine Crest Boulders. American Geophysical Union, Fall Meeting, 2018AGUFMEP53F1959H, 2018, abstract #EP53F-1959.

Harrison, S., Winchester, V., Glasser, N.F., 2007. The timing and nature of recession of outlet glaciers of Hielo Patagonico Norte, Chile, from their Neoglacial IV (Little Ice Age) maximum positions. Global Planet. Change 59 (1–4), 67–78.

Huggel, C., Kääb, A., Haeberli, W., Teysseire, P., Paul, F., 2002. Remote sensing based assessment of hazards from glacierlake outbursts: a case study in the Swiss Alps. Can. Geotech. J. 39, 316–330.

Huh, K.I., Mark, B.G., Ahn, Y., Hopkinson, C., 2017. Volume change of tropical Peruvian glaciers from multi-temporal digital elevation models and volume-surface area scaling. Geogr. Ann. Phys. Geogr. 99 (3), 222–239.

Huh, K.I., Baraer, M., Mark, B.G., Ahn, Y., 2018. Evaluating glacier volume changes since the Little ice age maximum and consequences for stream flow by integrating models of glacier flow and hydrology in the Cordillera Blanca, Peruvian Andes. Water 10 (12), 1732.

Huss, M., Bookhagen, B., Huggel, C., Jacobsen, D., Bradley, R.S., Clague, J.J., Vuille, M., Buytaert, W., Cayan, D.R., Greenwood, G., Mark, B.G., Milner, A.M., Weingartner, R., Winder, M., 2017. Toward mountains without permanent snow and ice. Earths Future 5, 418–435.

IGM, 1975. Mapa geologico del Peru 1:1,000,000. Instituto de Geologia y Mineria (IGM), 1p.

Immerzeel, W.W., Lutz, A.F., Andrade, M., Bahl, A., Biemans, H., Bolch, T., Hyde, S., Brumby, S., Davies, B., Dahe, Q., Elmore, A.C., Emmer, A., Feng, M., Fernandez Rivera, A., Haritashya, U., Kargel, J.S., Koppes, M., Kulkarni, A.V., Mayewski, P., Nepal, S., Pacheco, P., Painter, T., Pellicciotti, F., Rajaram, H., Rupper, S., Sinisalo, A., Shrestha, A.B., Viviroli, D., Wada, Y., Xiao, C., Yao, T., Baillie, J., 2020. Importance and vulnerability of world's water towers. Nature 577, 364–369.

Innes, J.L., 1983. Use of aggregated Rhizocarpon species in lichenometry – an evaluation. Boreas 12 (3), 183–190.

Innes, J.L., 1985. Lichenometry. Prog. Phys. Geogr. 9 (2), 187–254.
INRENA, 2005. Plano general topografico y batimetrico de la laguna Lejiacocha, 1:2,000. Ministerio de Agricultura, Instituto Nacional de Recursos Naturales (INRENA), 1p.
IPCC, 2019. Special report on the ocean and cryosphere in a changing climate. Intergovernmental panel on climate change. Available from. https://www.ipcc.ch/srocc/.
Jomelli, V., Grancher, D., Brunstein, D., Solomina, O., 2008. Recalibration of the yellow Rhizocarpon growth curve in the Cordillera Blanca (Peru) and implications for LIA chronology. Geomorphology 93 (3–4), 201–212.
Jomelli, V., Favier, V., Rabatel, A., Brunstein, D., Hoffmann, G., Francou, B., 2009. Fluctuations of glaciers in the tropical Andes over the last millennium and palaeoclimatic implications: a review. Palaeogeogr. Palaeoclimatol. Palaeoecol. 181 (3–4), 269–282.
Jomelli, V., Favier, V., Vuille, M., Braucher, R., Martin, L., Blard, P.-H., Colose, C., Brunstein, D., He, F., Khodri, M., Bourles, D.L., Leanni, L., Rinterknecht, V., Grancher, D., Francou, B., Ceballos, J.L., Fonseca, H., Liu, Z., Otto-Bliesner, B.L., 2014. A major advance of tropical Andean glaciers during the Antarctic cold reversal. Nature 513 (7517), 224–228.
Jomelli, V., Martin, L., Blard, P.H., Favier, V., Vuillé, M., Ceballos, J.L., 2017. Revisiting the Andean tropical glacial behavior during the Antarctic cold reversal. Cuadernos Invest. Geogr. 43, 629–648.
Kinzl, H., 1942. Gletscherkundliche Begleitworte zur Karte der Cordillera Blanca (Peru). Z. Gletscherkd. 28 (1/2), 1–19.
Kinzl, H., Schneider, E., 1950. Cordillera Blanca, Peru. Universitats-Verlag Wagner, Innsbruck, p. 167.
Klimeš, J., Novotný, J., Novotná, I., Jordán de Urries, B., Vilímek, V., Emmer, A., Strozzi, T., Kusák, M., Cochachin Rapre, A., Hartvich, F., Frey, H., 2016. Landslides in moraines as triggers of glacial lake outburst floods: example from Palcacocha Lake (Cordillera Blanca, Peru). Landslides 13, 1461–1477.
Linsbauer, A., Paul, F., Haeberli, W., 2012. Modeling glacier thickness distribution and bed topography over entire mountain ranges with glabtop: application of a fast and robust approach. J. Geophys. Res. Earth Surf 117, 1–17.
López-Moreno, J.I., Navarro, F., Izagirre, E., Alonso, E., Rico, I., Zabalza, J., Revuelto, J., 2020. glacier and climate evolution in the pariacacá mountains, Peru. Cuadernos de Investigación Geográfica 46, 127–139.
Magnin, F., Haeberli, W., Linsbauer, A., Deline, P., Ravanel, L., 2020. Estimating glacier-bed overdeepenings as possible sites of future lakes in the de-glaciating Mont Blanc massif (Western European Alps). Geomorphology, 106913.
Mark, B., Stansell, N., Zeballos, G., 2017. The last deglaciation of Peru and Bolivia. Cuadernos de Investigación Geográfica 43, 591–628.
Martin, L.C.P., Blard, P.-H., Lavé, J., Jomelli, V., Charreau, J., Condom, T., Lupker, M., Arnold, M., Aumaître, G., Bourlès, D.L., Keddadouche, K., 2020. Antarctic-like temperature variations in the Tropical Andes recorded by glaciers and lakes during the last deglaciation. Quat. Sci. Rev. 247, 106542.
Matthews, J.A., 2005. Little Ice Age' glacier variations in Jotunheimen, southern Norway: a study in regionally controlled lichenometric dating of recessional moraines with implications for climate and lichen growth rates. Holocene 15 (1), 1–19.
McCarroll, D., 1991. The age and origin of neoglacial moraines in Jotunheimen, Southern Norway – new evidence from weathering-based data. Boreas 20 (3), 283–295.
Moon, BP, 1984. Refinement of a technique for determining rock mass strength for geomorphological purposes. Earth Surf. Process. Landforms 9 (2), 189–193.
Muñoz, R., Huggel, C., Frey, H., Cochachin, A., Haeberli, W., 2020. Glacial lake depth and volume estimation based on a large bathymetric dataset from the Cordillera Blanca, Peru. Earth Surf. Process. Landforms. https://doi.org/10.1002/esp.4826.
Osborn, G., Taylor, J., 1975. Lichenometry on calcareous substrates in Canadian Rockies. Quat. Res. 5 (1), 111–120.
Osborn, G., McCarthy, D., LaBrie, A., Burke, R., 2015. Lichenometric dating: Science or pseudo-science? Quat. Res. 83 (1), 1–12.
Rabatel, A., Francou, B., Jomelli, V., Naveau, P., Grancher, D., 2008. A chronology of the Little Ice Age in the tropical Andes of Bolivia (16 degrees S) and its implications for climate reconstruction. Quat. Res. 70 (2), 198–212.
Rabatel, A., Francou, B., Soruco, A., Gomez, J., Caceres, B., Ceballos, J.L., Basantes, R., Vuille, M., Sicart, J.E., Huggel, C., Scheel, M., Lejeue, Y., Arnaud, Y., Collet, M., Condom, T., Consoli, G., Favier, V., jomeli, V., Galarraga, R., Ginot, P., Maisincho, L., mendoza, J., Menegoz, M., Ramirez, E., Ribstein, P., Suarez, W., Villacis, M., Wagnon, P., 2013. Current state of glaciers in the tropical Andes: a multi-century perspective on glacier evolution and climate change. Cryosphere 7 (1), 81–102.
Racoviteanu, A.R., Arnaud, Y., Williams, M., Ordoñez, J., 2008. Decadal changes in glacier parameters in the Cordillera Blanca, Peru, derived from remote sensing. J. Glaciol. 54 (186), 499–510.
Reynolds Geo-Sciences, 2003. Development of glacial hazard and risk minimisation protocols in rural environments. In: Methods of Glacial Hazard Assessment and Management in the Cordillera Blanca, Peru. Reynolds Geo-Sciences Ltd., Flintshire (UK), p. 72.
Rodbell, D.T., 1992. Lichenometric and radiocarbon dating of Holocene glaciation, Cordillera Blanca, Peru. Holocene 2 (1), 19–29.
Rodbell, D.T., Seltzer, G.O., 2000. Rapid ice margin fluctuations during the younger Dryas in the tropical Andes, 0 Quat. Res. 54 (3), 328–338.
Rosenwinkel, S., Korup, O., Landgraf, A., Dzhumabaeva, A., 2015. Limits to lichenometry. Quat. Sci. Rev. 129, 229–238.
Sattar, A., Goswami, A., Kulkarni, A.V., Das, P., 2019. Glacier-surface velocity derived ice volume and retreat assessment in the dhauliganga basin, central himalaya–A remote sensing and modeling based approach. Front. Earth Sci. 7, 105.
Scherler, D., Leprince, S., Strecker, M.R., 2008. Glacier-surface velocities in alpine terrain from optical satellite imagery-Accuracy improvement and quality assessment. Remote Sens. Environ. 112, 3806–3819.
Schoeneich, P., 1998. Les stades tardiglaciaires des Préalpes vaudoises et leur corrélation avec le modèle des Alpes orientales. *ETHZ*. VAW Mitteilungen 158, 192–207.
Schoolmeester, T., Johansen, K.S., Alfthan, B., Baker, E., Hesping, M., Verbist, K., 2018. Atlas de Glaciares y Aguas Andinos. El impacto del retroceso de los glaciares sobre los recursos hídricos. UNESCO, Arendal, France, p. 77p.
Seltzer, G.O., 1992. Late quaternary glaciations of the Cordillera real, Bolivia. J. Quat. Sci. 7, 87–98.
Silverio, W., Jaquet, J.-M., 2017. Evaluating glacier fluctuations in Cordillera Blanca (Peru) by remote sensing between 1987 and 2016 in the context of ENSO. Arch. Sci. 69, 145–162.
Smith, J.A., Rodbell, D.T., 2010. Cross-cutting moraines reveal evidence for North Atlantic influence on glaciers in the tropical Andes. J. Quat. Sci. 25 (3), 243–248. https://doi.org/10.1002/jqs.1393.
Solomina, O., Calkin, P.E., 2003. Lichenometry as applied to moraines in Alaska, USA, and kamchatka, Russia. Arctic Antarct. Alpine Res. 35 (2), 129–143.
Solomina, O., Jomelli, V., Kaser, G., Ames, A., Berger, B., Pouyaud, B., 2007. Lichenometry in the Cordillera Blanca, Peru: "Little ice age'' moraine chronology. Global Planet. Change 59 (1–4), 225–235.
Stansell, N.D., Licciardi, J.M., Rodbell, D.T., Mark, B.G., 2017. Tropical ocean-atmospheric forcing of late glacial and Holocene glacier fluctuations in the Cordillera Blanca, Peru. Geophys. Res. Lett. 44 (9), 4176–4185.
Taggart, J.R., 2009. Master's Theses and Capstones. Developing a 'Little Ice Age' Glacial Chronology in the Southern Peruvian Andes Using Lichenometry and Cosmogenic Beryllium-10 Surface Exposure Dating, vol. 498. https://scholars.unh.edu/thesis/498.
Thompson, L., Mosley-Thompson, E., Henderson, K., 2000. Ice-core paleoclimaterecords in tropical South America since the last glacial maximum. J. Quat. Sci. 15, 107–115.
Úbeda, J., de Marcos, J., Vásquez, E., Concha, R., Masías, P., Bustamante, M., Gómez, R., Iparraguirre, J., Schimmelpfennig, I., Braucher, R., Barrientos, Í., Luna, G., Astete, I., 2019. El registro cosmogénico glacial del cambio climático en los Andes peruanos: resultados del proyecto FONDECYT 144-2015. Simposio ‚Las Montañas Nuestro Futuro'. Cuzco, Perú 10–12 december 2019.
USGS, 2019. LandsatLook viewer of the United States geological survey. available from URL, accessed: August to September 2019. https://landsatlook.usgs.gov/viewer.html.
Veettil, B.K., 2018. Glacier mapping in the Cordillera Blanca, Peru, tropical Andes, using sentinel-2 and Landsat data. Singapore J. Trop. Geogr. 39, 351–363.
Veettil, B.K., Kamp, U., 2017. Remote sensing of glaciers in the tropical Andes: a review. Int. J. Rem. Sens. 38, 7101–7137.
Veliz, J.B., Oberti, L.I., Fernandez, E.R., 1975. Estudio tecnico para determinar el grado de peligrosidad de la Laguna Lajiacocha. ELECTROPERÚ: Huaráz, Peru, p. 24p.
Vuille, M., Francou, B., Wagnon, P., Juen, I., Kaser, G., mark, B.G., Bradley, R.S., 2008. Climate change and tropical Andean glaciers: past, present and future. Earth Sci. Rev. 89 (3–4), 79–96.
Vuille, M., Carey, M., Huggel, C., Buytaert, W., Rabatel, A., Jacobsen, D., Soruco, A., Villacis, M., Yarleque, C., Elison Timm, O., Condom, T., Salzmann, N., Sicart, J.-E., 2018. Rapid decline of snow and ice in the tropical Andes – impacts, uncertainties and challenges ahead. Earth Sci. Rev. 176, 195–213.
Winchester, V., Harrison, S., 2000. Dendrochronology and lichenometry: colonization, growth rates and dating of geomorphological events on the east side of the North Patagonian Icefield, Chile. Geomorphology 34 (3–4), 181–194.
Winchester, V., Harrison, S., Warren, C.R., 2001. Recent retreat Glaciar Nef, Chilean Patagonia, dated by lichenometry and dendrochronology. Arctic Antarct. Alpine Res. 33 (3), 266–273.
Zemp, M., Huss, M., Thibert, E., Eckert, N., McNabb, R., Huber, J., Barandun, M., Machguth, H., Nussbaumer, S.U., Gärtner-Roer, I., Thomson, L., Paul, F., Maussion, F., Kutuzov, S., Cogley, J.G., 2019. Global glacier mass changes and their contributions to sea-level rise from 1961 to 2016. Nature 568 (3), 382–386.